Received: 29 November 2019 | Revised: 27 May 2020 | Accepted: 6 July 2020

DOI: 10.1111/mec.15556

ORIGINAL ARTICLE

MOLECULAR ECOLOGY WILEY

Odorant binding proteins promote flight activity in the migratory insect, *Helicoverpa armigera*

Shang Wang[1,2] | Melissa Minter[2,3] | Rafael A. Homem[2] | Louise V. Michaelson[4] | Herbert Venthur[5,6] | Ka S. Lim[2] | Amy Withers[7] | Jinghui Xi[1] | Christopher M. Jones[2,8] | Jing-Jiang Zhou[1,2]

[1]College of Plant Sciences, Jilin University, Changchun, China

[2]Biointeractions and Crop Protection, Rothamsted Research, Harpenden, UK

[3]Department of Biology, University of York, York, UK

[4]Plant Sciences, Rothamsted Research, Harpenden, UK

[5]Laboratorio de Química Ecológica, Departamento de Ciencias Químicas y Recursos Naturales, Universidad de La Frontera, Temuco, Chile

[6]Centro de Investigación Biotecnológica Aplicada al Medio Ambiente (CIBAMA), Universidad de La Frontera, Temuco, Chile

[7]Lancaster Environment Centre, Lancaster University, Lancaster, UK

[8]Vector Biology Department, Liverpool School of Tropical Medicine, Liverpool, UK

Correspondence
Christopher M. Jones, Vector Biology Department, Liverpool School of Tropical Medicine, Pembroke Place, Liverpool, L3 5QA, UK.
Email: chris.jones@lstmed.ac.uk

Jing-Jiang Zhou, College of Plant Sciences, Jilin University, Changchun, Jilin Province 130062, China.
Email: jjzhouchina@163.com

Funding information
Jilin University, Grant/Award Number: TAQ(JZ)-2017[7]-201811; Biotechnology and Biological Sciences Research Council, Grant/Award Number: BB/N012011/1 and BBS/E/C/000I0420

Abstract

Migratory insects are capable of actively sustaining powered flight for several hours. This extraordinary phenomenon requires a highly efficient transport system to cope with the energetic demands placed on the flight muscles. Here, we provide evidence that the role of the hydrophobic ligand binding of odorant binding proteins (OBPs) extends beyond their typical function in the olfactory system to support insect flight activity via lipid interactions. Transcriptomic and candidate gene analyses show that two phylogenetically clustered OBPs (OBP3/OBP6) are consistently over-expressed in adult moths of the migrant Old-World bollworm, *Helicoverpa armigera*, displaying sustained flight performance in flight activity bioassays. Tissue-specific over-expression of *OBP6* was observed in the antennae, wings and thorax in long-fliers of *H. armigera*. Transgenic *Drosophila* flies over-expressing an *H. armigera* transcript of OBP6 (HarmOBP6) in the flight muscle attained higher flight speeds on a modified tethered flight system. Quantification of lipid molecules using mass spectrometry showed a depletion of triacylglyerol and phospholipids in flown moths. Protein homology models built from the crystal structure of a fatty acid carrier protein identified the binding site of OBP3 and OBP6 for hydrophobic ligand binding with both proteins exhibiting a stronger average binding affinity with triacylglycerols and phospholipids compared with other groups of ligands. We propose that HarmOBP3 and HarmOBP6 contribute to the flight capacity of a globally invasive and highly migratory noctuid moth, and in doing so, extend the function of this group of proteins beyond their typical role as chemosensory proteins in insects.

KEYWORDS

Helicoverpa, insect migration, odorant binding proteins

1 | INTRODUCTION

Insect flight is one of the most energetically demanding processes in the animal kingdom. Long-distance insect migrants can actively sustain periods of flight for several hours. To achieve these remarkable feats of endurance, migratory insects have evolved a suite of morphological, sensory and physiologically traits that form part of an inherited "migratory syndrome" (Dingle, 2014; Liedvogel, Akesson, & Bensch, 2011; Roff & Fairbairn, 2007). Comparative genomics and quantitative trait analyses reveal considerable genetic variation for single migratory traits but the associated molecular genetic mechanisms and biochemical pathways remain poorly understood.

The vital role of chemical cues in host location and oviposition (Bruce & Pickett, 2011; Hansson & Stensmyr, 2011; Mescher & De Moraes, 2015) means that the involvement of a sophisticated olfactory system in migration and flight ability is an attractive proposition (Getahun et al., 2016; McCormick et al., 2017). For example, the odorant receptor family (OR), central to the olfactory system of pterygotes, emerged prior to the evolution of winged flight in insects as an adaptation to terrestrial life (Brand et al., 2016). New evidence suggests that OR-based signal transduction in *Drosophila* is necessary for efficient odour localization in flight (Getahun et al., 2016). Our recent transcriptomic work (RNA sequencing [RNA-seq]) in the Old World bollworm, *Helicoverpa armigera*, has shown that specific odorant binding proteins (OBPs), OBP3 and OBP6, are highly and consistently over-expressed in moths displaying sustained flight activity (Jones et al., 2015). This suggests that OBPs have a direct or indirect role in supporting insect flight and their function extends beyond their part in host-seeking and mating behaviour.

Insect OBPs are small, water-soluble extracellular transporter proteins (13–16 kDa; Lartigue et al., 2002; Tegoni, Campanacci, & Cambillau, 2004; Zhou, 2010), and possess extreme diversity between species with as little as 8% amino acid conservation (Pelosi, Zhou, Ban, & Calvello, 2006; Zhou, He, Pickett, & Field, 2008). They are generally thought to contribute to the sensitivity of the olfactory system by participating in the binding, solubilization and transportation of hydrophobic ligands through the sensillum lymph of the antennae (Grosse-Wilde, Svatos, & Krieger, 2006; Leal, 2013; Tsuchihara et al., 2005) and in protecting odours from enzymatic degradation (Chertemps et al., 2012; Gomez-Diaz, Reina, Cambillau, & Benton, 2013). Some OBPs, however, are found in nonchemosensory tissues and may participate in other physiological processes (Graham et al., 2001; Guo et al., 2011; Missbach, Vogel, Hansson, & Grosse-Wilde, 2015; Pelosi et al., 2006). The *Drosophila* OBP28a is not required for odorant transport and signal transduction, implying a different function altogether (Larter, Sun, & Carlson, 2016). The homologues of OBP6 and OBP3 in *H. armigera* are highly expressed in nonolfaction tissues in other noctuid moths, *Agrotis ipsilon* and *Helicoverpa assulta* (Gu et al., 2014; Li et al., 2015). In arthropods, OBPs are found exclusively in insects (Pelosi, Iovinella, Felicioli, & Dani, 2014) and comparative genomics suggests that the evolution of this protein family provided a mechanism to mediate the transport of hydrophobic chemical signals present in a terrestrial environment (Vieira & Rozas, 2011).

The Noctuidae family of moths possess some of the most important and polyphagous agricultural insect pests globally. A key characteristic that makes them such devastating pests is their ability to spread hundreds of kilometres in response to deteriorating local conditions. This exacerbates their potential to invade new territories, as observed with the current fall armyworm (*Spodoptera frugiperda*), which has spread eastwards into the Asian continent and the rapid expansion of *H. armigera* in the Americas following its recent incursion (Fitt, 1989; Jones, Parry, Tay, Reynolds, & Chapman, 2019). Adult moths from both species can climb to high altitudes and sustain active flight for several hours (Chapman et al., 2010). This requires an enormous amount of fuel consumption, metabolism and intracellular transport to the flight muscles. Given the well-established hydrophobic binding capacity of OBPs and their over-expression in *H. armigera*, it is possible that this group of proteins act as lipid transport carriers in *H. armigera*—the main flight fuel of migratory insects (Van der Horst & Ryan, 2012).

In the present study, we use a combination of behavioural, molecular, transgenic and protein modelling approaches to (a) determine the tissue-specificity of two OBPs consistently expressed in *H. armigera* adult moths demonstrating sustained flight activity, (b) show that the transgenic overexpression of one of these OBPs leads to enhanced flight performance in *Drosophila*, (c) identify the primary lipids depleted in *H. armigera* following flight and (d) identify the key residues responsible for lipid binding. Overall, our findings provide evidence that a subset of OBPs are responsible for binding key lipids commonly used by insect migrants and that this relationship promotes insect flight.

2 | MATERIALS AND METHODS

2.1 | *Helicoverpa armigera* strains

The adult *Helicoverpa armigera* used in this study originated from a long-term laboratory strain, *Bayer* (courtesy of the Max Planck Institute), and a wild-caught population from Spain (courtesy of the University of Valencia). The moths used in the RNA-seq were from a colony established from northern Greece. Insects were reared under a constant light regime of 14:10 hr light–dark at 26 ± 1°C in the insectaries of Rothamsted Research and the flight mill trials were conducted under the same conditions. Larvae were reared individually in 37-ml clear plastic pots containing a chickpea artificial diet and allowed to pupate before transfer to clean pots filled with vermiculite. Adult emergence was checked daily and any emerged individuals were set aside for flight mill trials or for rearing onto the next generation.

2.2 | Flight propensity of *H. armigera* measured by tethered flight mill

A series of flight mill experiments were conducted to determine the effects of over-expression of candidate genes associated with

migration or flight in *H. armigera* displaying contrasting flight abilities. A detailed description of the flight mill system is explained elsewhere (Jones et al., 2015; Minter et al., 2018). Insects from *Bayer* and *Spain* strains were reared through at least one generation in the insectary prior to flight mill trials and each strain was flown in independent experiments. Adult moths assigned to flight mill trials were placed at 4–10°C to facilitate the attachment of ~60-mg pins to the thorax with adhesive glue. Each moth was provided with 10% honey water solution ad libitum prior to flight. Moths were attached randomly to one of 16 flight mills via a pin and allowed to rest on a paper platform until the first flight was initiated by the insect. All flights took place between 7 p.m. and 9 a.m. under a 10-hr dark cycle from 8 p.m. to 6 a.m. At ~9 a.m. the next morning, individuals were taken off the mills and placed into individual pots for weighing. Any dead, unhealthy (e.g., broken wings or damage through improper handling) or escaped individuals were recorded and excluded from further analyses. All individuals were snap-frozen or placed in RNAlater within 2 hr and stored at −80°C for downstream molecular analysis.

The aggregated response variables were calculated for all individuals. We considered four response variables as being important discriminants of "strong" and "weak" fliers based on previous experiments; total distance flown (m), average speed flown (m/s), maximum speed attained (m/s) and number of bouts. Seven individuals from each strain were selected for RT-qPCR (reverse transcriptase quantitative polymerase chain reaction) of candidate genes from the ends of the flight activity distribution based on total distance and number of flight bouts.

2.3 | Tissue-specific candidate gene expression profiling in *H. armigera* flown on the flight mills

Initially, we determined the expression of 20 candidate genes from the head and thorax of 28 individual moths flown on the mills. The head (including the antennae) and thorax were removed using dissection instruments and placed in separate Eppendorf tubes with lysis buffer. The samples were homogenized using pellet pestles (Sigma-Aldrich). RNA was extracted using an Isolate II RNA Mini Kit (Bioline) and RNA was eluted in RNase-free water. cDNA was synthesized from 230 ng total RNA using SuperScript IV Reverse Transcriptase (Invitrogen) and Oligo$(dT)_{20}$ (Invitrogen).

Twenty candidate genes were screened for gene expression levels. qPCR primers were screened over a five-fold serial dilution of a cDNA sample (1/10th to 1/6,000th) and the primer efficiency was calculated. qPCRs were completed on the RotorGene 6000 (Qiagen) with conditions of 95°C for 2 min, followed by 40 cycles of 95°C for 10 s, 57°C for 15 s and 72°C for 20 s, followed by a melt curve analysis. Each reaction contained 10 μl of SYBR Green JumpStart Taq ready mix (Sigma-Aldrich), 300 nm of each primer and 5 μl of cDNA (1/50th dilution). The control genes *β-actin* and *elongation factor 1-α* were used for normalization (Wang, Dong, Desneux, & Niu, 2013; Yan et al., 2013) and all reactions were run in duplicate. Ct values were adjusted for primer pair efficiency. Expression levels were compared using a two-sided *t* test on the dCt values ($p < .05$) and are presented as $\log_{10}$ fold-change using ddCt (Schmittgen & Livak, 2008). RNA-seq was performed on moths flown and not-flown ($N = 4$ per group) according to previously described methods (Jones et al., 2015). All genes were considered significantly expressed at a false discovery rate of $p < .1$.

Following the identification of strong OBP expression profiles from the 20 candidate genes we determined the tissue-specific expression of OBP6 in the antennae, heads, thoraces, abdomens, legs and wings of *H. armigera* flown on the flight mills. Tissues were dissected from 18 adults and promptly immersed in liquid nitrogen and stored at −80°C. RNA was extracted using RNA-Solv reagent (Omega) following the manufacturer's protocol. Total RNA was quantified and checked for purity and integrity using a NanoDrop 2000 Spectrophotometer (Thermo Fisher Scientific) and gel electrophoresis. HiScript II Q RT SuperMix for qPCR with gDNA wiper (R223-01; Vazyme) was used for cDNA synthesis.

For tissue-specific expression profiling, RT-qPCR primer pairs were designed using PRIMER 5 software (Untergasser et al., 2012) and the same control genes used as above. mRNA levels were measured by RT-qPCR using the ChamQTM SYBR qPCR Master Mix (Vazyme). Each amplification reaction contained 1 μl synthesized cDNA, 10 μl of 2× ChamQTM SYBR qPCR Master Mix, 0.4 μl of 10 μm forward primer, 0.4 μl reverse primer and 8.2 μl water in a 20-μl reaction mix. Reactions were performed on an ABI 7500 Real-Time PCR System (Applied Biosystems) under the following conditions: 30 s denaturation at 95°C and 40 cycles of 95°C for 10 s and 60°C for 30 s, followed by a melt curve for specificity analysis. Fold-change values were calculated from the mean of three biological replicates with the ddCt method and using the abdomen as the calibrator. Relative expression levels were compared using the dCt values ($p < .05$) as described above.

2.4 | Quantitative triacylglycerol analysis

Total lipids were extracted from moth tissue ground in liquid nitrogen (Usher et al., 2017). The molecular species of triacylglycerols (TAGs) were analysed by electrospray ionization triple quadrupole mass spectrometry (ESI-MS; using API 4000 QTRAP; Applied Biosystems). TAGs are defined by the presence of one acyl fragment and the mass/charge of the ion formed from the intact lipid (neutral loss profiling; Krank, Murphy, Barkley, Duchoslav, & McAnoy, 2007). This allowed identification of one TAG acyl species and the total acyl carbons and total number of acyl double bonds in the other two chains. The procedure does not allow identification of the other two fatty acids individually nor the positions (sn-1, sn-2 or sn-3) that individual acyl chains occupy on the glycerol. TAG was quantified after background subtraction, smoothing, integration, isotope deconvolution and comparison of sample peaks with those of the internal standard (using LipidView, AB-Sciex). The profiling samples were prepared by combining 10 μl of the total lipid extract with 990 μl of isopropanol/methanol/50 mm ammonium acetate/dichloromethane (4:3:2:1). Samples

were infused at 15 μl/min with an autosampler (LC mini PAL, CTC Analytics). The scan speed was 100 μ s^{-1}. The collision energy, with nitrogen in the collision cell, was set to +25 V; declustering potential +100 V; entrance potential 14 V; and exit potential +14 V. Sixty continuum scans were averaged in the multiple channel analyser mode. For product ion analysis, the first quadrupole mass spectrometer (Q1) was set to select the TAG mass and Q3 for the detection of fragments produced by collision-induced dissociation. The mass spectral responses of various TAG species are variable, owing to differential ionization of individual molecular TAG species. For all analyses gas pressure was set on "low," and the mass analysers were adjusted to a resolution of 0.7 μm full width height. The source temperature was set to 100°C, the interface heater was deployed, +5.5 kV applied to the electrospray capillary; the curtain gas was set at 20 (arbitrary units); and the two ion source gases were set at 45 (arbitrary units). The data were normalized to the internal standard Tri15:0 (Sigma Aldrich) and further normalized to the weight of the initial sample.

2.5 | Quantitative phospholipid analysis

Quantitative analyses to measure phospholipids (PL), phosphatidylcholine (PC), phosphatidylethanolamine (PE), phosphatidylinositol (PI), phosphatidylglycerol (PG) and phosphatidylserine (PS) were carried out using electrospray ionization tandem triple-quadrupole mass spectrometry (API 4000 QTRAP; Applied Biosystems; ESI-MS/MS). The lipid extracts were diluted and resuspended in $CHCl_3$/MeOH/300 mm ammonium acetate in water, 300:665:35. Internal standards were obtained and quantified as previously described (Devaiah et al., 2006). Samples were directly infused at 15 μl/min with an autosampler (HTS-xt PAL, CTC-PAL Analytics). Data acquisition and acyl group identification of the polar lipids was performed, with modifications, from Ruiz-Lopez, Haslam, Napier, and Sayanova (2014). The internal standards were supplied by Avanti, incorporated as 0.085 nmol di24:1-PC, 0.08 nmol di14:0-PE, 0.08 nmol di18:0-PI, 0.032 nmol di18:0-PS and 0.08 nmol di14:0-PG.

The molecular species of polar lipids were defined on the basis of the presence of a head-group fragment and the mass/charge of the intact lipid ion formed by ESI. However, tandem ESI-MS/MS precursor and product ion scanning, based on head group fragment, did not determine the individual fatty acyl species. Instead, polar lipids were identified at the level of class, total acyl carbons and total number of acyl carbon–carbon double bonds.

The data were processed using the program LIPID VIEW SOFTWARE (AB-Sciex) where isotope corrections are applied. The peak area of each lipid was normalized to the internal standard and further normalized to the weight of the initial sample. A parametric two-sided *t* test was used to compare lipid content between flown and not flown moths ($N = 4–5$ moths per group).

2.6 | Phylogenetic analysis of *H. armigera* OBPs

N-terminal signal peptides of OBPs were predicted by signal ip 4.0 (http://www.cbs.dtu.dk/services/SignalP/). Alignment of amino acid sequences (without signal peptides) was performed by mafft (https://www.ebi.ac.uk/Tools/msa/mafft/). The phylogenetic trees of OBPs were constructed using MEGA6 software by the maximum-likelihood method with 1,000 bootstraps with the *p*-distance model (Gong, Zhang, Zhao, Xia, & Xiang, 2009).

2.7 | Development of a novel flight mill for *Drosophila melanogaster* and other small insects

We designed a new set of flight mills to accommodate smaller insects to examine the flight ability of wild type and transgenic *Drosophila* flies (Figure S1). These flight mills are similar in structural design to those used in the *H. armigera* experiments, comprising a flight arm and rotational disc to allow flies to move around an axis by means of a very low-friction magnetic bearing (Figure S1).

As part of the study we developed a robust standard operating procedure for tethering *Drosophila*. Briefly, an individual fly was lightly anaesthetized with CO_2 and transferred to a custom-made paper groove which had been made to allow accurate positioning of an anaesthetized fly (Figure S1). The paper groove was placed on the platform with CO_2 passing through the groove bottom. When the flies were under CO_2 anaesthesia, the tip of a small flight mill arm (a 5-cm-long, 0.2-mm-diameter copper wire) was tethered onto the dorsal side of the anaesthetized fly's thorax with Super Glue under a stereomicroscope (Olympus SZ40). Individual flies and the small flight mill arms were gently handled with either a small brush or jeweller's vacuum tweezers. Once the glue was dry and hard, the tethered flies were moved to the experimental chamber, fed with sucrose solution from a small piece of filter paper and allowed to rest in the recording chambers to adapt to the experimental environment overnight prior to data collection. At 10 a.m. the following day, filter papers were removed from the recording chambers and data collection was started using the same software as the larger mills. Experiments were run until ~2.30 p.m. to ensure each mill had run for at least 3 hr. Any flies which looked damaged, unhealthy or had escaped from the flight arm were disregarded from further analyses.

2.8 | Generation of transgenic *Drosophila* expressing *HarmOBP6*

All *Drosophila* strains were maintained on standard food (Bloomington formulation) at 24°C and 65% relative humidity on a 12/12-hr light/dark cycle. Proteinase K treatment and phenol/chloroform extraction were used to isolate genomic DNA (gDNA) from adult *D. melanogaster* flies for use in PCR.

HarmOBP6 (B5X24_HaOG200803 with the addition of a stop codon) was codon-optimized for expression in *D. melanogaster* and synthetized by GeneArt (ThermoFisher Scientific). The codon-optimized sequence was transferred from the subcloning plasmid pMA (GeneArt) to the attB-carrying plasmid pUAST (pUASTattB_EF362409) using restriction enzymes *Eco*RI and *Xho*I. The pUAST-*Harm-OBP6* construct was microinjected into syncytial blastoderm

embryos of an integration strain (y w M[eGFP, vas-int, dmRFP]ZH-2A; Pattp40; Dundas et al., 2006) that carries an *attP* docking site on the second chromosome (*attP40*) and the *phiC31* integrase gene under control of a germline-specific (*vasa*) promoter on the X chromosome. This strain was sourced from the Fly Facility, University of Cambridge. The GAL4 strain (w[1118]; Pw[+mW.hs] = GawBDJ757) was sourced from Bloomington Drosophila Stock Centre (BDSC-8184). Microinjections were performed in-house using an inverted microscope (eclipse TieU Nikon) equipped with a 10×/0.25 lens, 10×/22 eyepiece and fluorescence illumination. Injection mixtures consisted of 0.5× phosphate buffer (pH 6.8, 0.05 mm sodium phosphate, 2.5 mm KCl), 300 ng/μl of the pUAST-*Harm-OBP6* construct and 200 mg/L fluorescein sodium salt and delivered by a FemtoJet express micro-injector (Eppendorf) controlled by a motorized micromanipulator (TransferMan NK2; Eppendorf). Injection needles were prepared following Miller, Holtzman, and Kaufman (2002).

Micro-injection survivors were back-crossed and the F_1 progeny was screened for the presence of the *white* marker gene (orange eye phenotype). Positive flies were intercrossed to generate homozygous flies (red eyes) which were selected to establish the final strain. Control flies carrying an empty pUAST plasmid (*UAS-empty* strain) were generated following the same protocols described above.

2.9 | Tethered flight of transgenic *Drosophila* and statistical analysis of flight response variables

Three flight mill experiments were performed to compare the flight ability of transgenic *Drosophila* flies carrying *HarmOBP6* (GAL4 > UAS-OBP6 line) with control flies (GAL4 > UAS line). In addition, we were also interested in how flight activity changes with the age of the fly. A total of eight flies were flown simultaneously per run with each trial consisting of a mixture of *HarmOBP* and control flies.

1. Experiment 1: flies generated from crosses between male *UAS-OBP6* (*UAS-empty* for controls) and female *muscle-GAL4* strains. *GAL4 > UAS-OBP6* virgin females ($N = 28$) were flown on the mills alongside *GAL4 > UAS* virgin female control flies ($N = 28$). The age of the flies in this experiment ranged from 24 to 144 hr after emergence.
2. Experiment 2: flies were generated from crosses between female *UAS-OBP6* (*UAS-empty* for controls) and male *muscle-GAL4*. Both *GAL4 > UAS-OBP6* ($N = 23$) and *GAL4 > UAS* control ($N = 21$) female flies were mated prior to the flight mill trials. Flies were either 2, 6 or 15 days old after emergence.
3. Experiment 3: *GAL4 > UAS-OBP6* ($N = 43$) and *GAL4 > UAS* ($N = 34$) control flies were generated as in Experiment 2 but without mating. The age of the flies ranged from 7 to 26 days old after emergence.

After preliminary trials, we determined that a 1-hr cut-off period was sufficient to measure flight performance with difference between the average speeds attained between 1 and 3 hr of flight (example from Experiment 3 in Figure S2). We were primarily interested in the two response variables, the average speed flown (AVGSP; m/s) and maximum speed attained (MAXSP; m/s). We hypothesized that the average or maximum speed of flight is a much more useful metric to distinguish the flight activity of flies such as *Drosophila* because they are not capable of sustaining hours of flight like larger insects (e.g., Lepidoptera). The distribution of each flight parameter was assessed using the FITDIST package (Delignette-Muller & Dutang, 2015) using QQ plots and goodness of fit statistics. AVGSP and MAXSP were both normally distributed (Figure S2).

Data were fitted using generalized linear mixed models (GLMMs) using the LME4 package in R (Bates, Machler, Bolker, & Walker, 2015). To model AVGSP and MAXSP as a function of the covariates we used a Gaussian linear mixed-effects model. Fixed covariates were *strain* (transgenic or control) and *age* (categorical). An interaction term *strain* × *age* was included. To incorporate differences between the flight mills on which the individual was flown we included *mill* as a random effect. Best-fit GLMMs were created using a backward stepwise approach from the maximally complex model, which included the interaction. Explanatory variables were retained in the best-fit model according to significance ($p < .05$) in likelihood ratio tests (LRTs). Model assumptions were verified using residual-fitted plots. Predictions of response variables from each model were made using least square means (LSMs) in the package LSMEANS (Lenth, 2016) and differences between groups assessed using Tukey post hoc tests.

2.10 | Homology structure modelling of *H. armigera* OBPs

The amino acid sequences of HarmOBP6 and HarmOBP3 were used as a target while the template was the crystal structure of the blowfly *Phormia regina* OBP56a (PregOBP56a) (PDB code: 5DIC). The pheromone binding protein 1 from the silkmoth *Bonbyx mori* BmorPBP1 (1DQE) was used as the template for HarmPBP1 structure modelling. Five hundred models of each OBP were obtained using MODELLER9.14 (http://salilab.org/modeller) and the best initial model was selected according to the lowest discrete optimized protein energy (DOPE) score provided by the software. The stereochemistry of the best model was assessed using the theoretical validation package PROCHECK (Laskowski, Macarthur, Moss, & Thornton, 1993), and the overall structure was visualized using PYMOL software (http://www.pymol.org). Further refinement steps were carried out with NAMD version 2.9 (parallel molecular dynamics code for biomolecular system simulation) installed in the high-performance computer (HPC) Lautaro Linux cluster at Centro de Modelación y Computación Científica (CMCC) from Universidad de La Frontera. The CHARMM36 (Huang et al., 2016) force field was used for all the simulations. The selected protein model was solved with the TIP3P water model in a cubic box with a minimum distance of 10 Å between the protein and the edge of the box. Neutralization of the protein–water system was performed by adding Na^+ or Cl^- randomly placed in the box. Likewise, the system was simulated under periodic boundary conditions with a cutoff radius of 12 Å for nonbonded interactions and a time step of 2 fs. Alpha-carbons (Cα) of secondary structures were fixed with a constant force of 1 kcal/mol $Å^{-1}$. A first energy minimization of 10,000

steps was performed followed by heating through short simulations of 1 ps at 50, 100, 150, 200, 250 and 300 K. Long simulations were kept at 300 K and 1 bar pressure in the NTP (referred to a constant number of particles, temperature and pressure) over 50 ns. A root-mean-square deviation (RMSD) trajectory tool was used to calculate the RMSD with reference to the starting structure (Figure S3). Therefore, when the plotted RMSD showed small fluctuations (~1–1.5 Å), coordinates were analysed by PROCHECK every 100 frames to obtain the best structure (lowest energy). Finally, the putative binding site and its volume were calculated via the CASTp server (http://sts-fw.bioengr.uic.edu/castp/calculation.php; Dundas et al., 2006).

2.11 | Molecular docking

The refined structures of HarmOBP6 and HarmOBP3 were used as the target for molecular docking with AUTODOCK VINA (Trott & Olson, 2010). Likewise, a refined 3D structure of the pheromone binding protein HarmPBP1 was used as the reference template for the molecular docking tasks based on its reported function in binding sex pheromones (Dong et al., 2017; Ye et al., 2017). Energy minimization and optimization for the ligands used in this study were performed using MM2 minimization methods in the CHEM3D 16.0 Software (Perkin Elmer). For HarmOBP6, polar hydrogens were added using the interface AUTODOCK TOOLS, as well as torsional bonds for ligands. A grid box with $26 \times 26 \times 26$ points and a default space of 1 Å was prepared via AUTOGRID following the predicted binding site by the CASTp server. For every docking run, an exhaustiveness of 500 was considered and the best binding modes were selected according to the lowest free binding energy (kcal/mol). The TAGs and phospholipids were energy-minimized following the same protocol for fatty acids and semiochemicals. Considering that AUTODOCK VINA allows a maximum of 32 rotatable bonds, these compounds and their binding to HarmOBP6 and HarmOBP3 were submitted to the DINC server (http://dinc.kavrakilab.org/; Antunes et al., 2017; Dhanik, McMurray, & Kavraki, 2013). This server was used to dock the lipids into the HarmOBP6 and HarmOBP3 binding site following the above grid box parameters and with all rotatable bonds active. The DINC server allows docking for large molecules based on the AUTODOCK algorithm and fragmentation processes, for which fragments that show best binding are incrementally expanded by adding atoms of the ligand to it in each of several rounds. Thus, both fully flexible and bound conformations of lipid molecules were extracted and docked again into HarmOBP6, HarmOBP3 and HarmPBP1 (control) using AUTODOCK VINA.

3 | RESULTS AND DISCUSSION

3.1 | Two *Helicoverpa armigera*-specific OBPs are overexpressed in the thorax of moths displaying prolonged flight activity

Adult moths from two colonized strains of *Helicoverpa armigera* (*Bayer* and *Spain*) were flown overnight on a computerized tethered flight mill system that experimentally quantifies the flight performance of individual insects in the absence of external stimuli (Minter et al., 2018). Previous flight mill studies with noctuid moths have shown an inverse relationship between the total distance flown and the number of individual flight bursts to discriminate those insects engaging in prolonged or more appetitive behaviour (Jones et al., 2015). We used this relationship to assign individual moths into two distinct flight activity groups, "short-distance" (SD) or "long-distance" (LD), for downstream gene expression analyses (Figure 1a).

We undertook a candidate gene approach to determine the differential expression of 20 genes in the two strains of *H. armigera* flown on the flight mills. As a baseline control, and to validate some of our previously detected candidate genes from whole transcriptome studies (Jones et al., 2015), RNA-seq of moths flown and not flown on the flight mills was performed. Eight of our 20 candidate genes were significantly up-regulated in the flown group with OBP6 showing the highest and most consistent level of up-regulation (Figure S4). Each gene has a reported role in insect migration or sustained flight activity including those involved in circadian and photoreceptor processes (Reppert, Guerra, & Merlin, 2016), lipid metabolism (Arrese & Soulages, 2010), OBPs (Jones et al., 2015), flight muscle structure (Zhan et al., 2014), and the metabolism of proline and phenylalaine/tryptophan (Arrese & Soulages, 2010; Rio, Attardo, & Weiss, 2016; Figure 1b).

In the *Bayer* strain four genes were significantly over-expressed in the thorax of the LD moths, all of which were up-regulated exclusively in the thorax and not the head (Figure 1b; Table S1). These four genes encode two OBPs (*OBP3* and *OBP6*), the *protein henna-like isoform X3* and a *fatty-acid synthase-like* gene. In the thorax of individuals from the strain *Spain*, three genes were significantly over-expressed in the LD group; *myofilin*, *OBP3* and *protein henna-like isoform X3*; and three genes were significantly over-expressed in the SD group, *collagen alpha subunit-1(IV)*, *cry-1* and *phospholipase A2-like*. Two genes were differentially expressed in the head of *H. armigera* individuals from the *Spain* strain (although the magnitude of this expression was small; Figure 1b).

Following the detection of OBP over-expression both in this study and from transcriptome profile analysis (RNA-seq [Figure S4]; Jones et al., 2015), we showed that the relative expression levels of *OBP3* and *OBP6* in individual *H. armigera* displayed a significant positive correlation with flight performance which was strongest in the thorax (*HarmOBP3*: head: $R = 0.49$, $p = .006$, thorax: $R = 0.81$, $p < .001$; *HarmOBP6*: head: $R = 0.31$, $p = .18$, thorax: $R = 0.65$, $p = .002$; Figure 1c). Furthermore, we quantified the expression of *HarmOBP6* in the antenna, head, thorax, abdomen, leg and wing of SD and LD moths. *HarmOBP6* was significantly over-expressed in the antennae ($p = .016$), thoraces ($p = .009$) and wings ($p = .05$) and this expression was significantly up-regulated in LD moths compared with those in the SD group (Figure 1d; Table S2).

The simple phenotypic comparisons of SD and LD insects presented here provide a measurement of flight performance in terms of the raw physiological capacity to fly. We recognize that a full spectrum of flight behaviours exists and that these are controlled by intricate internal and external processes. For example, the migratory flight behaviour of the Monarch butterfly (*Danaus plexippus*)

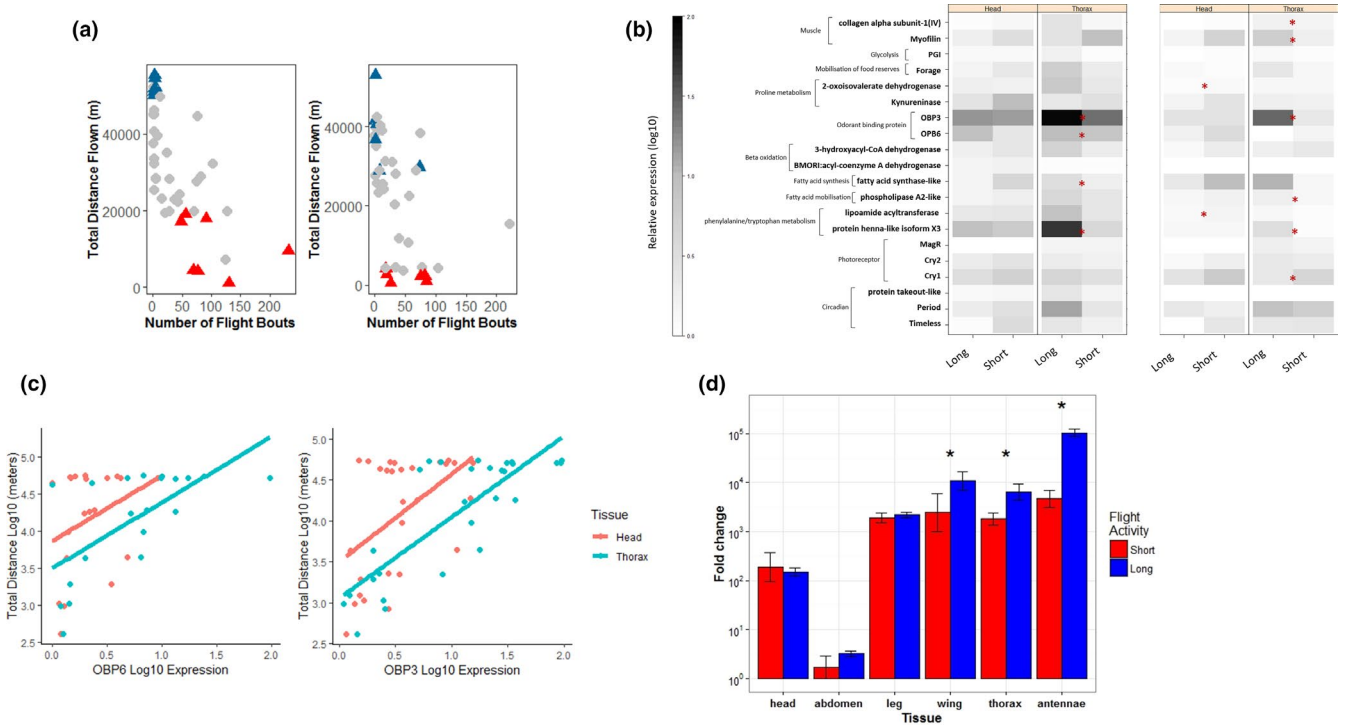

FIGURE 1 The expression of OBPs in adult *H. armigera* flown on tethered flight mills. (a) Flight activity of *H. armigera* moths characterized using tethered flight. Total distance flown and the number of flight bouts were used to discriminate moths displaying short-distance (red) or long-distance (blue) activity in two colonised strains, Bayer (left) and Spain (right). Individuals assigned to gene expression experiments denoted with a triangle. (b) A heatmap showing the RT-qPCR expression (log10) of twenty genes previously associated with migration and/or sustained flight activity in insects. Differential expression was determined between 'long' or 'short' fliers from the Bayer (left) and Spain strain (right). Genes are grouped by known physiological function. Expression levels were compared using a two-sided test on dCT values in the head and thorax and significance is denoted with the red * (non-adjusted $p < .05$). (c) The increase in OBP expression with flight performance measured by total distance flown (log10 metres). (d) Fold-change expression of OBP6 in six tissues from *H. armigera* flown on the flight mills. * represents significant differences in expression levels between flight groups ($p < .05$)

is controlled in response to environmental changes (temperature, photoperiod) via internal genetic, and possibly epigenetic, cascades (Merlin & Liedvogel, 2019). Here we focus on raw flight capacity and use our expression profiling to speculate on the functional role of OBPs in insect flight.

3.2 | Phylogenetic analysis of the odorant binding proteins implicated in *H. armigera* flight

An alignment of the protein sequences of HarmOBP3 (accession no.: AEB54582) and HarmOBP6 (accession no.: AEB54587) is provided in Figure S5. Based on the sequence alignment, HarmOBP6 belongs to the classic OBP subgroup, which contains typical characteristic sequence features of six conserved cysteine residues and the classic insect OBP motif: C_1-X_{15-39}-C_2-X_3-C_3-X_{21-44}-C_4-X_{7-12}-C_5-X_8-C_6 (Figure S5; Zhou et al., 2008). Phylogenetic analysis shows that HarmOBP3 and HarmOBP6 are clustered into the same branch with 100% bootstrap support between OBP3 and OBP6, indicating that they share a high homologous amino acid sequence similarity and probably a similar function (Figure S6). There is 81% amino acid identity between OBP3 and OBP6. HarmOBP6 is also closely clustered with other *Helicoverpa* OBPs such as *Helicoverpa assulta*, HassOBP6 (accession no.: AEX07270) and *Heliothis virescens*, HvirOBP0136 (accession no.: ACX53819; Figure S6).

3.3 | Transgenic *Drosophila* expressing OBP6 in the flight muscle attain higher speeds on a novel flight mill system

To functionally validate the role of OBPs in flight activity we generated a transgenic *D. melanogaster* strain that over-expresses *HarmOBP6* in muscle cells and assessed the performance of these flies on a newly designed flight mill system for small dipterans (Figure S1). We chose OBP6 based on its magnitude of expression in a Chinese strain of *H. armigera* previously reported as well as the flown/not flown comparison (Figure S4) but postulate that the high conservation between the protein sequences of OBP6 and OBP3 (see phylogenetic analysis above) would lead to similar results had we chosen OBP3. Transgenic strains were generated using the φC31 integration system (Bischof, Maeda, Hediger, Karch, & Basler, 2007). Genomic integration of *HarmOBP6* in generated transgenic flies, hereafter referred to as *UAS-OBP6* strain, was confirmed by PCR and sequencing (Figure 2a). The *GAL4/UAS* expression system (Brand & Perrimon, 1993) was used to induce the expression of *HarmOBP6* in

muscle cells by using a muscle-specific GAL4 driver strain (Seroude, Brummel, Kapahi, & Benzer, 2002) (referred to as *muscle-GAL4* strain). The over-expression of *HarmOBP6* in transgenic flies generated from the cross between the *UAS-OBP6* and *muscle-GAL4* strains (GAL4 > UAS-OBP6 flies) was confirmed by RT-PCR and RT-qPCR (Figure 2a). The expression of *HarmOBP6* increased by more than 15 times in *GAL4 > UAS-OBP6* flies when compared to parental *muscle-GAL4* and *UAS-OBP6* (Figure 2a).

We performed a series of flight mill experiments with three separate experimental trials. First, we compared the 1-hr flight activity of *Gal4 > UAS-OBP6* transgenic and *Gal4 > UAS* control flies. These flies are genetically identical, the only difference being the absence of *HarmOBP6* in the controls. The average and maximum speeds (m/s) attained during the 1 hr of flight activity were analysed using GLMMs as a function of the covariates strain and age (Table 1). There was no difference in the average or maximum speed between *Gal4 > UAS-OBP6* and *Gal4 > UAS* control flies when *Gal4 > UAS-OBP6* originated from crosses using *UAS-OBP6* as the male parent (Experiment 1, Table 1). In this experiment there was evidence for increased speeds in older (over 48 hr old) *Gal4 > UAS-OBP6* flies.

By contrast, *Gal4 > UAS-OBP6* flies originating from the reciprocal cross (*UAS-OBP6* as the female parent) flew consistently faster and attained higher maximum speeds than control flies (Figure 2b–e; Table 1) and this pattern was observed in both mated and virgin F_1 flies (Experiments 2 and 3). There was an effect of age in both experiments: flies from the older age groups (those flies emerging after 1 week) flew faster than the younger cohort. The discrepancy in the F_1 flight activity results between *UAS-OBP6* male and female parental lines could be due to maternal effects as observed in laboratory crosses of "short" and "long" flight phenotypes from other moth species (Gu & Danthanarayana, 1992).

3.4 | Quantification of TAG and phospholipids in flown *H. armigera*

We hypothesize that OBPs function as a fuel carrier for the supply of lipids to the flight muscles during prolonged flight in *H. armigera*. To determine candidate lipid molecular species for binding with OBPs we compared the total lipid content of age-matched moths flown on the flight mills with those reared to adults and not forced to undergo flight. Six lipid classes were assayed using ESI-MS including TAG, PE, PS, PI, PG and PC.

Unsurprisingly total TAG levels were (a) the most abundant class of the lipids analysed and (b) underwent the most pronounced decline in flown moths (1.8-fold reduction from 739.6 to 410.5 nmol/g fresh weight, $p = .006$; Figure 3a). Sustained flight activity in insects is powered primarily by the mobilization of TAG in the insect fat body into diacylglycerol (DAG), which is then shuttled in the haemolymph to the flight muscle (Van der Horst & Ryan, 2012).

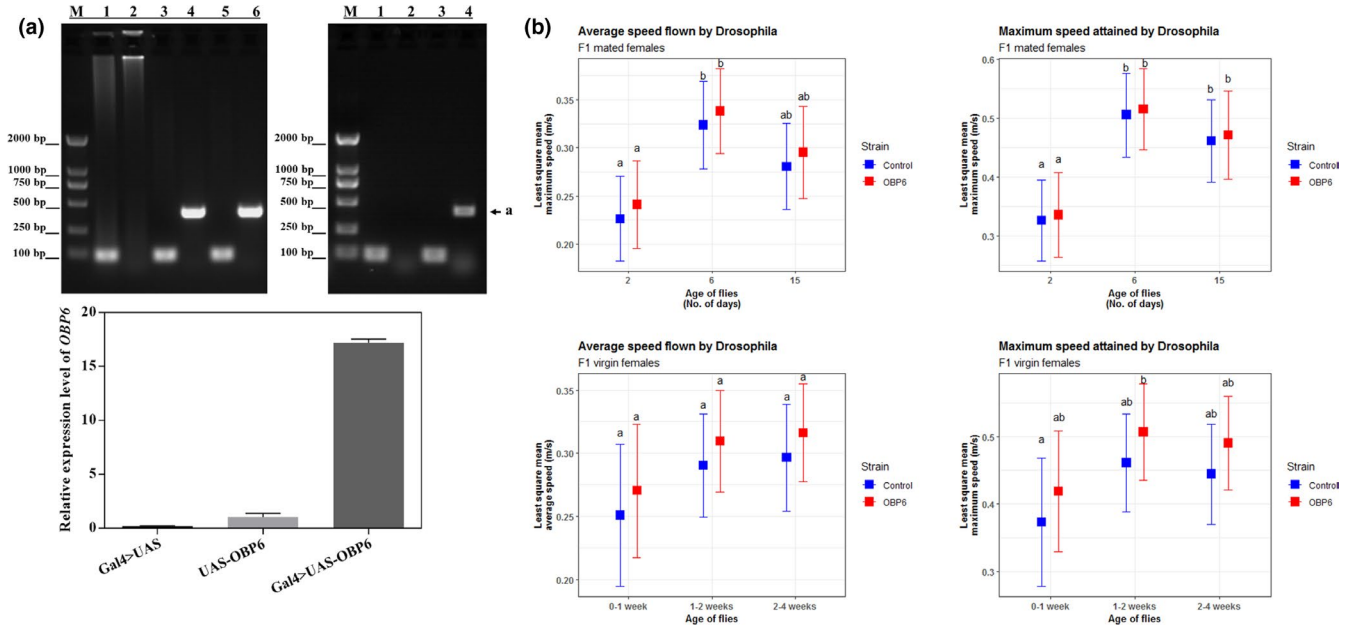

FIGURE 2 Effect of expression of *HarmOBP6* on Drosophila flight activity. (a) Genomic integration of HarmOBP6 into transgenic flies. (top panel) PCR products amplified from cDNA of transgenic flies. Lane 1, Rpl32 primers, control *GAL4>UAS* flies; Lane 2, OBP6 primers, control *GAL4>UAS* flies; Lane 3, Rpl32 primers, *GAL4>UAS-OBP6* female flies; Lane 4, OBP6 primers, *GAL4>UAS-OBP6* female flies; Lane 5, Rpl32 primers, *GAL4>UAS-OBP6* male flies; Lane 6, OBP6 primers, *GAL4>UAS-OBP6* male flies; M, DNA Maker. Symbol a indicates OBP6. (bottom panel) RT-qPCR of HarmOBP6 in *GAL4>UAS-OBP6* transgenic flies in comparison to GAL4>UAS and UAS-OBP6 control flies. (b) Flight activity bioassays with Drosophila expressing *HarmOBP6* with F1 virgin females (bottom row) and F1 mated feamles (top row). The average speed and maximum speed between transgenic and control Drosophila flies predicted using Least Square Means (LSMs) and differences between groups assessed using Tukey *post-hoc* tests. Results presented are for Experiment 2 (top row) and 3 (bottom row) with *Gal4>UAS-OBP6* flies originating from the reciprocal cross (*UAS-OBP6* as the female parent)

TABLE 1 Estimated regression parameters, standard errors and *t* values for GLMMs for *Drosophila* flight mill experiments

Experiment	Response	Regression parameter	Estimate	*SE*	*t* value
No. 1 F_0 = ♂*UAS-OBP6* × ♀*muscle-GAL4*	AVGSP	Intercept	0.316	0.021	14.70
F_1 = Virgin ♀		StrainOBP6	−0.019	0.026	−0.72
		AgeOver48h	0.048	0.026	1.84
	MAXSP	Intercept	0.481	0.033	12.35
		StrainOBP6	−0.017	0.035	−0.49
		AgeOver48h	0.067	0.037	1.84
No. 2 F_0 = ♀*UAS-OBP6* × ♂*muscle-GAL4*	AVGSP	Intercept	0.226	0.015	14.76
F_1 = Mated ♀		StrainOBP6	0.015	0.016	0.93
		Age6D	0.097	0.019	5.11
		Age15D	0.054	0.019	2.81
	MAXSP	Intercept	0.326	0.024	13.68
		StrainOBP6	0.010	0.025	0.40
		Age6D	0.179	0.030	6.05
		Age15D	0.135	0.030	4.50
No. 3 F_0 = ♀*UAS-OBP6* × ♂*muscle-GAL4*	AVGSP	Intercept	0.251	0.020	12.50
F_1 = Virgin ♀		StrainOBP6	0.019	0.015	1.34
		Age2weeks	0.039	0.021	1.90
		Age4weeks	0.046	0.021	2.22
	MAXSP	Intercept	0.373	0.034	11.03
		StrainOBP6	0.046	0.024	1.95
		Age2weeks	0.088	0.034	2.62
		Age4weeks	0.071	0.033	2.14

Note: AVGSP is the average speed and MAXSP is the maximum speed flown on the flight mill.

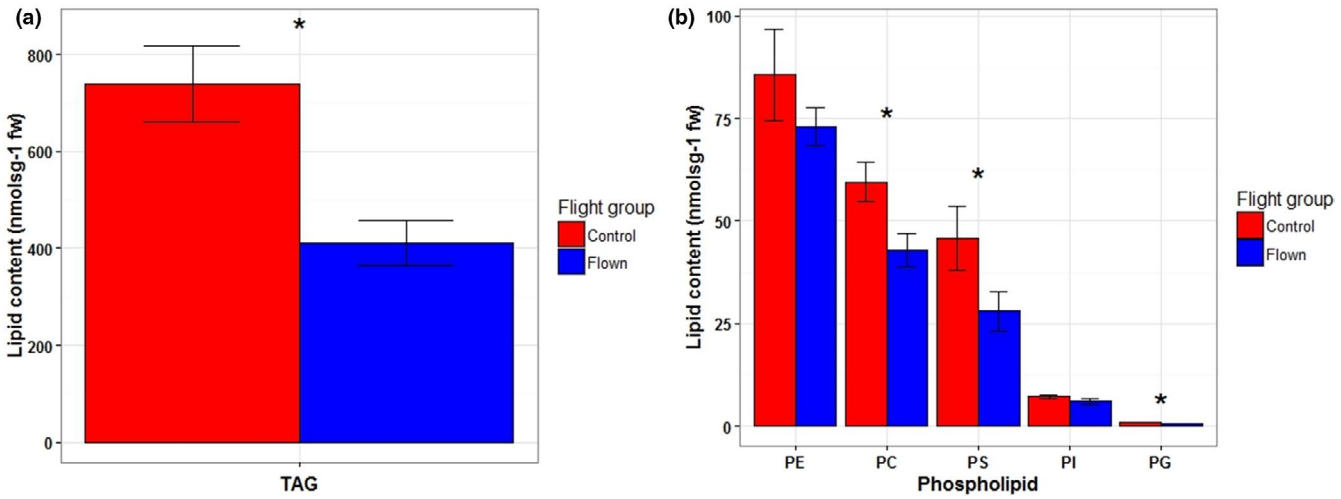

FIGURE 3 Lipid depletion in flown *H. armigera* measured by electrospray ionization tandem triple-quadrupole mass spectrometry (ESI-MS). (a) Total triacylglycerol (TAG) (nmolesg-1 per fresh weight (FW) content in flown versus control *H. armigera*. (b) Depletion of five phospholipid classes in flown moths; phosphatidylethanolamine (PE), phosphatidylserine (PS), phosphatidylinositol (PI), phosphatidylglycerol (PG) and phosphatidylcholines (PC). Error bars represent SE (n = 4-5 per group) and * indicates significant differences ($p < .05$) between flight groups

The role of phospholipid metabolism in insects is far less well understood although in this experiment we show a consistent depletion in each phospholipid class following flight (Figure 3b; see Figure S7 for individual lipid species and Table S3 for test statistics). In mammals the relative abundance of the two most common phospholipids, PC and PE (also the two most abundant classes in *H. armigera* moths measured by ESI-MS, Figure 3b), regulates the size and dynamics of lipid droplets and energy metabolism (Veen

et al., 2017). Phospholipids are critical to membrane structure and function; the fatty acyl components of the phospholipids can provide another potential energy source. When cells are subject to starvation, levels of phospholipid classes decrease (Steinhauser et al., 2018). Lipid droplets are storage organelles at the centre of lipid and energy homeostasis. They have a unique architecture consisting of a hydrophobic core of neutral lipids which is dominated by TAG, enclosed by a phospholipid monolayer that is decorated by a specific set of proteins (Olzmann & Carvalho, 2019). Utilizing the reserves of TAG from lipid droplets for energy will release phospholipids, which can also be metabolized.

3.5 | The protein structure and lipid binding site of *H. armigera* OBPs

We used the 3D structure of an OBP from the blowfly, *Phormia regina* (PregOBP56a; Ishida, Ishibashi, & Leal, 2013), as a template for HarmOBP6 and HarmOBP3, and the pheromone binding protein from the silkmoth *Bombyx mori* BmorPBP1 (1DQE) as a template for HarmPBP1, to build structural models and predict the binding efficacy to a range of fatty acids. We used HarmPBP1 as a positive control for semiochemical binding in relation to its observed role in female sex pheromone response (Ye et al., 2017). As expected, the structures of both HarmOBP6 and HarmOBP3 resemble typical insect OBPs, consisting of six α-helices connected by loops and three disulphide bridges that contribute to overall structural stability (Figures 4a and S8). Binding site prediction indicates the OBP has a pocket of 772.8 $Å^3$ volume and 917.1 $Å^2$ area for OBP6 and 777.9 $Å^3$ volume and 642.4 $Å^2$ area for OBP3 with a "Tunnel" conformation suitable for lipid binding (Figures 4b and S8).

To quantify the strength of molecular interactions between the over-expressed OBPs and potential substrates, molecular docking was conducted to determine binding energies with a range of fatty acids and olfactory odorants (semiochemicals; Table 2). A total of 33 compounds were selected to dock with the predicted HarmOBP6, HarmOBP3 and HarmPBP1 protein structures, including nine fatty acids, 15 semiochemicals (identified from the Pherobase database https://www.pherobase.com), L-proline (amino acid; Rio et al., 2016), D-trelahose (sugar) and a selection of DAG/TAG/phospholipid species analysed by ESI-MS (Table 2).

The *H. armigera* OBPs possessed the lowest overall binding energies with TAG and phospholipids (Table 2). Apart from PE, HarmOBP3 had a greater binding affinity to each long-chain lipid than OBP6, with mean docking values for modelled HarmOBP6 and HarmOBP3 of −16.30 ± 0.80 and −18.20 ± 1.84 kcal/mol respectively. The lowest values were observed for HarmOBP3:TAG (52:2) and HarmOBP:phosphatidylinositol (PI 36:3; Table 2). The predicted binding model for PI in the pocket of OBP3 and OBP6 is shown in Figure 4c) with optimal predictions for TAG and other phospholipids in Figure S8. In contrast, the binding predictions between HarmPBP1 and lipid molecules were highly inconsistent (Table 2). As expected from its putative role in sex pheromone transportation (Ye et al., 2017), HarmPBP1 bound semiochemicals and fatty acids with greater negative values compared to the OBPs (Table 2). There was little difference in semiochemical or fatty acid docking values between OBP6 and OBP3. Overall, these molecular docking patterns support the hypothesis that the *H. armigera* OBPs investigated in

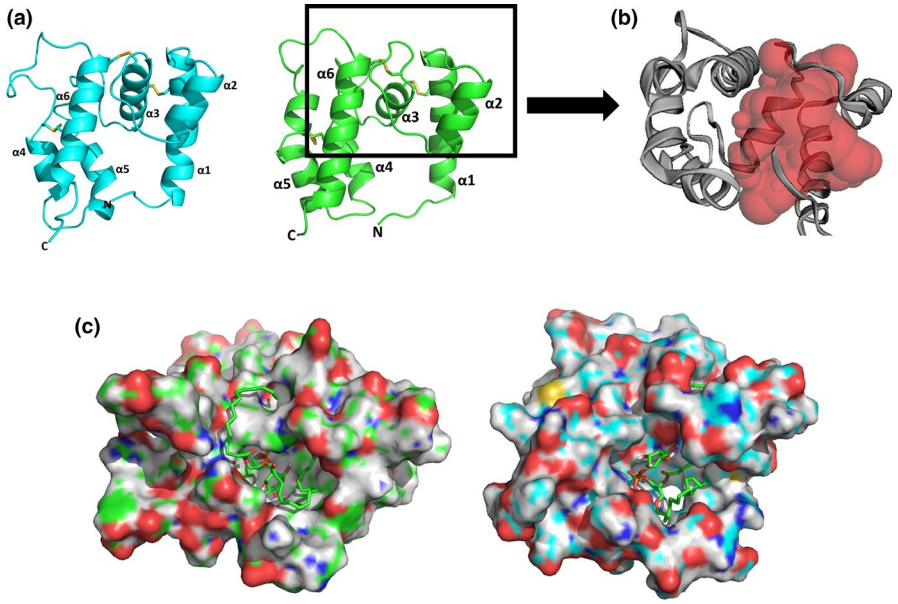

FIGURE 4 Predicted 3D-homolgy models of *H. armigera* OBPs and optimised docking predictions for phosphatidylinositol. (a) Protein helices for OBP3 (cyan) and OBP6 (green) are shown with disulfide bridges indicated by yellow sticks. C- and N-termini are highlighted with C and N, respectively. Alpha-helix domains are highlighted with "α" and corresponding numbers. (b) The binding site prediction of OBP6 using CASTp. Red surface indicates the pocket with 772.8 Å3 of volume and 917.1 Å2 of area. (c) Docking prediction of phosphatidylinositol (PI) with OBP3 (left) and OBP6 (right). This phospholipid had the lowest estimated free-energy of binding with both OBPs from AutoDock

TABLE 2 Molecular docking between HarmOBP6 and HarmOBP3 with fatty acids, semiochemicals, triacylglycerols (TAG) and phospholipids

		Binding energy (kcal/mol)		
Ligand	**Ligand**	**OBP6**	**OBP3**	**PBP1[a]**
Fatty acids	1,2-diacylglycerol	−5.1	−4.6	−4.9
	α-linolenic acid	−5.8	−5.7	−7.8
	cis-vaccenic acid	−5.6	−5.3	−6.9
	D-trehalose	−5.2	−5.5	−5.5
	γ-linolenic acid	−6.2	−5.7	−7.5
	Linoleic acid	−5.4	−5.3	−7.3
	L-proline	−4.5	−4.4	−4.5
	Oleic acid	−5.4	−5.5	−7.0
	Palmitic acid	−5.3	−5.1	−6.5
	Palmitoleic acid	−5.5	−5.9	−6.9
	Stearic acid	−5.6	−5.5	−6.7
	trans-vaccenic acid	−5.5	−6.0	−7.1
Semiochemicals	2-phenylacetaldehyde	−5.1	−4.6	−5.9
	2-phenylethanol	−4.9	−4.7	−5.8
	benzaldehyde	−4.8	−4.6	−5.6
	heptanal	−4.2	−3.9	−4.6
	hexadecanal	−5.0	−4.9	−6.5
	hexadecanol	−5.0	−4.8	−6.3
	nonanal	−4.7	−3.9	−5.4
	phenylmethanol	−4.7	−4.8	−5.4
	salicylaldehyde	−5.0	−5.0	−5.2
	tetradecanal	−5.0	−4.5	−6.0
	(*Z*)-7-hexadecenal	−5.2	−5.0	−6.7
	(*Z*)-9-hexadecenal	−5.5	−5.0	−6.6
	(*Z*)-9-tetradecenal	−5.2	−4.8	−6.4
	(*Z*)-11-hexadecenal	−5.4	−4.9	−6.7
	(*Z*)-11-hexadecenol	−5.3	−5.0	−6.4
TAG/phospholipid	triacylglycerol—TAG (52:3)	−13.0	−21.0	−7.5
	triacylglycerol—TAG (52:2)	−18.0	−22.0	50.8
	phosphatidylethanolamine—PE (36:4)	−17.5	−3.8	5.1
	phosphatidylserine—PS (36:2)	−18.0	−19.4	19.1
	phosphatidylinositol—PI (36:3)	−19.9	−21.4	26.0
	phosphatidylglycerol—PG (34:3)	−17.6	−18.7	21.3
	phosphatidylcholines—PC (36:5) (1)[b]	−13.7	−18.2	−0.7
	phosphatidylcholines—PC (36:5) (2)	−14.0	−19.3	−14.8
	phosphatidylcholines—PC (36:5) (3)	−15.3	−19.7	−1.5

[a]HarmPBP1 used as reference target with a reported function in binding sex pheromones.

[b]Numbers in parentheses indicate isomers for phosphatidylcholines as carbon atoms:unsaturations. (1) represents 18:3/18:2; (2) represents 18:2/18:3 and (3) represents 16:0/20:5.

this study have a binding affinity for long-chain fatty acids which is either supplementary to their role in olfaction or represents an entirely new physiological function. There is now compelling evidence that OBPs perform physiological functions beyond olfaction (Pelosi, Iovinella, Zhu, Wang, & Dani, 2018). The sensilla of *Drosophila* maintain a robust response to a wide range of odours even when all abundantly expressed antennal OBP genes are deleted, demonstrating that many OBPs are not essential to the olfactory response (Xiao,

Sun, & Carlson, 2019). Humidity detection (hygrosensation) relies on a single OBP (OBP59a) within *Drosophila* antenna (Sun et al., 2018), contravening the typical model that OBPs exclusively transport hydrophobic odorants to receptors. The diverse array of nonolfactory roles for OBPs in Diptera include bacterial-induced haematopoiesis in tsetse flies (Benoit et al., 2017), the transportation of sex-pheromones in *Helicoverpa* sp. (Sun, Huang, Pelosi, & Wang, 2012) and eggshell formation in the mosquito *Aedes aegypti* (Marinotti et al., 2014). The degree of redundancy in OBP function and the circumstances under which dual or split roles are performed is currently unknown, but tissue-specific functional genomics will undoubtedly begin to uncover the broader range of operation of OBPs.

4 | SUMMARY

It has recently become accepted that the versatility of OBPs is greater than previously thought and this group of proteins represent a highly adaptive set of hydrophobic carriers performing multiple physiological functions beyond their classical role in chemoreception (Pelosi et al., 2018). Our findings on two *Helicoverpa armigera* OBPs are consistent with this view and we propose an additional physiological role in regulating insect flight in a migratory Lepidopteran organism. The affinity of OBPs for long-chain fatty acids (Ishida et al., 2013) lends support to the hypothesis that OBPs act as carriers of hydrophobic free fatty acids produced from upstream lipid metabolism as part of the flight fuel pathway. The OBP homology structure models and binding affinities for a range of substrates described here support this. The precise mechanism(s) of how over-expressed OBPs contribute to flight performance at the biochemical and cellular level needs further study. Coping with the extreme energy demands of sustained migratory flight in insects is just one of several traits that make up the heritable "migratory syndrome" (Roff & Fairbairn, 2007). Investigating the pathways and mechanisms that support such a fascinating feat of endurance is an excellent means to understand animal migration at the genetic level.

ACKNOWLEDGEMENTS

We thank the three anonymous reviewers for their critical comments and suggestions for improvement of the initial draft. The Max Planck Institute in Jena, Germany, and the University of Valencia provided vital *Helicoverpa armigera* insect material. This work was supported by the UK Biotechnology and Biological Sciences Research Council (BBSRC) as part of a Future Leader Fellowship (grant no.: BB/N012011/1) (to C.M.J.) and by Jilin University, China. As part of a Tang Aoqing Chair Professorship (no. TAQ(JZ)-2017[7]-201811) to J.J.Z. L.V.M. is supported by the BBSRC Institute Strategic Programme Tailoring Plant Metabolism (BBS/E/C/000I0420).

AUTHOR CONTRIBUTIONS

C.M.J. and J.J.Z. conceived and designed the study. S.W., M.M., R.A.H., L.V.M. and H.V. performed the experimental work. K.S.L. designed and provided the tethered flight mill equipment. C.M.J., J.J.Z., S.W., A.W., M.M., L.V.M. and H.V. conducted data analysis. J.X. provided advice, academic and financial support for S.W. C.M.J. and J.J.Z. wrote the initial draft of the manuscript. All authors edited and made comments on the final draft.

DATA AVAILABILITY STATEMENT

The candidate gene qPCR, OBP6 tissue-specific expression and lipid quantification ESI-MS data have been archived in Dryad (https://doi.org/10.5061/dryad.dr7sqv9w4). The R script used to analyse the flight mill data is available on request from C.M.J.

ORCID

Rafael A. Homem https://orcid.org/0000-0001-9649-1825
Christopher M. Jones https://orcid.org/0000-0002-6504-6224

REFERENCES

Antunes, D. A., Moll, M., Devaurs, D., Jackson, K. R., Lizée, G., & Kavraki, L. E. (2017). DINC 2.0: A new protein-peptide docking webserver using an incremental approach. *Cancer Research*, *77*(21), E55–E57.

Arrese, E. L., & Soulages, J. L. (2010). Insect fat body: Energy, metabolism, and regulation. *Annual Review of Entomology*, *55*, 207–225. https://doi.org/10.1146/annurev-ento-112408-085356

Bates, D., Machler, M., Bolker, B. M., & Walker, S. C. (2015). Fitting linear mixed-effects models using lme4. *Journal of Statistical Software*, *67*(1), 1–48.

Benoit, J. B., Vigneron, A., Broderick, N. A., Wu, Y., Sun, J. S., Carlson, J. R., … Weiss, B. L. (2017). Symbiont-induced odorant binding proteins mediate insect host hematopoiesis. *eLife*, *6*, e19535. https://doi.org/10.7554/eLife.19535

Bischof, J., Maeda, R. K., Hediger, M., Karch, F., & Basler, K. (2007). An optimized transgenesis system for Drosophila using germ-line-specific phi C31 integrases. *Proceedings of the National Academy of Sciences of the United States of America*, *104*(9), 3312–3317.

Brand, A. H., & Perrimon, N. (1993). Targeted gene-expression as a means of altering cell fates and generating dominant phenotypes. *Development*, *118*(2), 401–415.

Brand, P., Robertson, H. M., Lin, W., Pothula, R., Klingeman, W. E., Jurat-Fuentes, J. L., & Johnson, B. R. (2016). The origin of the odorant receptor gene family in insects. *Elife*, *7*, e38340.

Bruce, T. J. A., & Pickett, J. A. (2011). Perception of plant volatile blends by herbivorous insects—Finding the right mix. *Phytochemistry*, *72*(13), 1605–1611. https://doi.org/10.1016/j.phytochem.2011.04.011

Chapman, J. W., Nesbit, R. L., Burgin, L. E., Reynolds, D. R., Smith, A. D., Middleton, D. R., & Hill, J. K. (2010). Flight orientation behaviors promote optimal migration trajectories in high-flying insects. *Science*, *327*(5966), 682–685. https://doi.org/10.1126/science.1182990

Chertemps, T., François, A., Durand, N., Rosell, G., Dekker, T., Lucas, P., & Maïbèche-Coisne, M. (2012). A carboxylesterase, Esterase-6, modulates sensory physiological and behavioral response dynamics to pheromone in Drosophila. *Bmc Biology*, *10*, 56. https://doi.org/10.1186/1741-7007-10-56

Delignette-Muller, M. L., & Dutang, C. (2015). fitdistrplus: An R Package for Fitting Distributions. *Journal of Statistical Software*, *64*(4), 1–34.

Devaiah, S. P., Roth, M. R., Baughman, E., Li, M., Tamura, P., Jeannotte, R., … Wang, X. (2006). Quantitative profiling of polar glycerolipid species from organs of wild-type Arabidopsis and a phospholipase D alpha 1 knockout mutant. *Phytochemistry*, *67*(17), 1907–1924.

Dhanik, A., McMurray, J. S., & Kavraki, L. E. (2013). DINC: A new AutoDock-based protocol for docking large ligands. *BMC Structural Biology*, *13*, S11. https://doi.org/10.1186/1472-6807-13-S1-S11

Dingle, H. (2014). *Migration: The biology of life on the move*, 2nd ed. Oxford, UK: Oxford University Press.

Dong, K., Sun, L., Liu, J. T., Gu, S. H., Zhou, J. J., Yang, R. N., … & Zhang, Y. J. (2017). RNAi-induced electrophysiological and behavioral changes reveal two pheromone binding proteins of Helicoverpa armigera involved in the perception of the main sex pheromone component Z11–16:Ald. *Journal of Chemical Ecology*, *43*(2), 207–214. https://doi.org/10.1007/s10886-016-0816-6

Dundas, J., Ouyang, Z., Tseng, J., Binkowski, A., Turpaz, Y., & Liang, J. (2006). CASTp: Computed atlas of surface topography of proteins with structural and topographical mapping of functionally annotated residues. *Nucleic Acids Research*, *34*, W116–W118. https://doi.org/10.1093/nar/gkl282

Fitt, G. P. (1989). The ecology of Heliothis species in relation to agroecosystems. *Annual Review of Entomology*, *34*, 17–52. https://doi.org/10.1146/annurev.en.34.010189.000313

Getahun, M. N., Thoma, M., Lavista-Llanos, S., Keesey, I., Fandino, R. A., Knaden, M., … Hansson, B. S. (2016). Intracellular regulation of the insect chemoreceptor complex impacts odour localization in flying insects. *Journal of Experimental Biology*, *219*(21), 3428–3438. https://doi.org/10.1242/jeb.143396

Gomez-Diaz, C., Reina, J. H., Cambillau, C., & Benton, R. (2013). Ligands for pheromone-sensing neurons are not conformationally activated odorant binding proteins. *Plos Biology*, *11*(4), e1001546. https://doi.org/10.1371/journal.pbio.1001546

Gong, D. P., Zhang, H. J., Zhao, P., Xia, Q. Y., & Xiang, Z. H. (2009). The odorant binding protein gene family from the genome of silkworm, *Bombyx mori*. *BMC Genomics*, *10*(1), 332. https://doi.org/10.1186/1471-2164-10-332

Graham, L. A., Tang, W., Baust, J. G., Liou, Y. C., Reid, T. S., & Davies, P. L. (2001). Characterization and cloning of a Tenebrio molitor hemolymph protein with sequence similarity to insect odorant-binding proteins. *Insect Biochemistry and Molecular Biology*, *31*(6–7), 691–702. https://doi.org/10.1016/S0965-1748(00)00177-6

Grosse-Wilde, E., Svatos, A., & Krieger, J. (2006). A pheromone-binding protein mediates the bombykol-induced activation of a pheromone receptor in vitro. *Chemical Senses*, *31*(6), 547–555. https://doi.org/10.1093/chemse/bjj059

Gu, H. N., & Danthanarayana, W. (1992). Quantitative genetic analysis of dispersal in *Epiphyas postvittana*. 1. Genetic variation in flight capacity. *Heredity*, *68*, 53–60.

Gu, S.-H., Sun, L., Yang, R.-N., Wu, K.-M., Guo, Y.-Y., Li, X.-C., … Zhang, Y.-J. (2014). Molecular characterization and differential expression of olfactory genes in the antennae of the black cutworm moth agrotis ipsilon. *PLoS One*, *9*(8), e103420. https://doi.org/10.1371/journal.pone.0103420

Guo, W., Wang, X., Ma, Z., Xue, L., Han, J., Yu, D., & Kang, L. (2011). CSP and takeout genes modulate the switch between attraction and repulsion during behavioral phase change in the migratory locust. *PLoS Genetics*, *7*(2), e1001291. https://doi.org/10.1371/journal.pgen.1001291

Hansson, B. S., & Stensmyr, M. C. (2011). Evolution of insect olfaction. *Neuron*, *72*(5), 698–711. https://doi.org/10.1016/j.neuron.2011.11.003

Ishida, Y., Ishibashi, J., & Leal, W. S. (2013). Fatty acid solubilizer from the oral disk of the blowfly. *PLoS One*, *8*(1), e51779. https://doi.org/10.1371/journal.pone.0051779

Jones, C. M., Papanicolaou, A., Mironidis, G. K., Vontas, J., Yang, Y., Lim, K. S., … Chapman, J. W. (2015). Genomewide transcriptional signatures of migratory flight activity in a globally invasive insect pest. *Molecular Ecology*, *24*(19), 4901–4911. https://doi.org/10.1111/mec.13362

Jones, C. M., Parry, H., Tay, W. T., Reynolds, D. R., & Chapman, J. W. (2019). Movement ecology of pest Helicoverpa: Implications for ongoing spread. *Annual Review of Entomology*, *64*, 277–295.

Huang, J., Rauscher, S., Nawrocki, G., Ran, T., Feig, M., De Groot, B. L., … & MacKerell, A. D. (2016). CHARMM36m: An improved force field for folded and intrinsically disordered proteins. *Nature Methods*, *14*(1), 71–73. https://doi.org/10.1038/nmeth.4067

Krank, J., Murphy, R. C., Barkley, R. M., Duchoslav, E., & McAnoy, A. (2007). Qualitative analysis and quantitative assessment of changes in neutral glycerol lipid molecular species within cells. *Methods in Enzymology*, *432*, 1–20.

Larter, N. K., Sun, J. S., & Carlson, J. R. (2016). Organization and function of Drosophila odorant binding proteins. *Elife*, *5*, e20242. https://doi.org/10.7554/eLife.20242

Lartigue, A., Campanacci, V., Roussel, A., Larsson, A. M., Jones, T. A., Tegoni, M., & Cambillau, C. (2002). X-ray structure and ligand binding study of a moth chemosensory protein. *Journal of Biological Chemistry*, *277*(35), 32094–32098. https://doi.org/10.1074/jbc.M204371200

Laskowski, R. A., Macarthur, M. W., Moss, D. S., & Thornton, J. M. (1993). PROCHECK—A programme to check the stereochemical quality of protein structures. *Journal of Applied Crystallography*, *26*, 283–291.

Leal, W. S. (2013). Odorant reception in insects: Roles of receptors, binding proteins, and degrading enzymes. *Annual Review of Entomology*, *58*, 373–391. https://doi.org/10.1146/annurev-ento-120811-153635

Lenth, R. V. (2016). Least-squares means: The R package lsmeans. *Journal of Statistical Software*, *69*(1), 1–33.

Li, Z.-Q., Zhang, S., Luo, J.-Y., Wang, C.-Y., Lv, L.-M., Dong, S.-L., & Cui, J.-J. (2015). Transcriptome comparison of the sex pheromone glands from two sibling Helicoverpa species with opposite sex pheromone components. *Scientific Reports*, *5*, 9324. https://doi.org/10.1038/srep09324

Liedvogel, M., Akesson, S., & Bensch, S. (2011). The genetics of migration on the move. *Trends in Ecology & Evolution*, *26*(11), 561–569. https://doi.org/10.1016/j.tree.2011.07.009

Marinotti, O., Ngo, T., Kojin, B. B., Chou, S. P., Nguyen, B., Juhn, J., … James, A. A. (2014). Integrated proteomic and transcriptomic analysis of the *Aedes aegypti* eggshell. *BMC Developmental Biology*, *14*, 15.

McCormick, A. C., Grosse-Wilde, E., Wheeler, D., Mescher, M. C., Hansson, B. S., & De Moraes, C. M. (2017). Comparing the expression of olfaction-related genes in gypsy moth (*Lymantria dispar*) adult females and larvae from one flightless and two flight-capable populations. *Frontiers in Ecology and Evolution*, *5*, 115. https://doi.org/10.3389/fevo.2017.00115

Merlin, C., &Liedvogel, M. (2019). The genetics and epigenetics of animal migration and orientation: Birds, butterflies and beyond. *Journal of Experimental Biology*, *222*, jeb191890. https://doi.org/10.1242/jeb.191890

Mescher, M. C., & De Moraes, C. M. (2015). Role of plant sensory perception in plant–animal interactions. *Journal of Experimental Botany*, *66*(2), 425–433. https://doi.org/10.1093/jxb/eru414

Miller, D. F. B., Holtzman, S. L., & Kaufman, T. C. (2002). Customized microinjection glass capillary needles for P-element transformations in *Drosophila melanogaster*. *BioTechniques*, *33*(2), 366–375.

Minter, M., Pearson, A., Lim, K. S., Wilson, K., Chapman, J. W., & Jones, C. M. (2018). The tethered flight technique as a tool for studying life-history strategies associated with migration in insects. *Ecological Entomology*, *43*(4), 397–411. https://doi.org/10.1111/een.12521

Missbach, C., Vogel, H., Hansson, B. S., & Grosse-Wilde, E. (2015). Identification of odorant binding proteins and chemosensory proteins in antennal transcriptomes of the jumping bristletail lepismachilis y-signata and the firebrat thermobia domestica: Evidence for an independent OBP-OR Origin. *Chemical Senses*, *40*(9), 615–626.

Olzmann, J. A., & Carvalho, P. (2019). Dynamics and functions of lipid droplets. *Nature Reviews Molecular Cell Biology*, *20*(3), 137–155. https://doi.org/10.1038/s41580-018-0085-z

Pelosi, P., Iovinella, I., Felicioli, A., & Dani, F. R. (2014). Soluble proteins of chemical communication: An overview across arthropods. *Frontiers in Physiology*, *5*, 320. https://doi.org/10.3389/fphys.2014.00320

Pelosi, P., Iovinella, I., Zhu, J., Wang, G. R., & Dani, F. R. (2018). Beyond chemoreception: Diverse tasks of soluble olfactory proteins in insects. *Biological Reviews*, *93*(1), 184–200. https://doi.org/10.1111/brv.12339

Pelosi, P., Zhou, J. J., Ban, L. P., & Calvello, M. (2006). Soluble proteins in insect chemical communication. *Cellular and Molecular Life Sciences*, *63*(14), 1658–1676. https://doi.org/10.1007/s00018-005-5607-0

Reppert, S. M., Guerra, P. A., & Merlin, C. (2016). Neurobiology of monarch butterfly migration. *Annual Review of Entomology*, *61*(1), 25–42. https://doi.org/10.1146/annurev-ento-010814-020855

Rio, R. V. M., Attardo, G. M., & Weiss, B. L. (2016). Grandeur alliances: Symbiont metabolic integration and obligate arthropod hematophagy. *Trends in Parasitology*, *32*(9), 739–749.

Roff, D. A., & Fairbairn, D. J. (2007). The evolution and genetics of migration in insects. *BioScience*, *57*(2), 155–164. https://doi.org/10.1641/B570210

Ruiz-Lopez, N., Haslam, R. P., Napier, J. A., & Sayanova, O. (2014). Successful high-level accumulation of fish oil omega-3 long-chain polyunsaturated fatty acids in a transgenic oilseed crop. *Plant Journal*, *77*(2), 198–208. https://doi.org/10.1111/tpj.12378

Schmittgen, T. D., & Livak, K. J. (2008). Analyzing real-time PCR data by the comparative C-T method. *Nature Protocols*, *3*(6), 1101–1108. https://doi.org/10.1038/nprot.2008.73

Seroude, L., Brummel, T., Kapahi, P., & Benzer, S. (2002). Spatio-temporal analysis of gene expression during aging in Drosophila melanogaster. *Aging Cell*, *1*(1), 47–56. https://doi.org/10.1046/j.1474-9728.2002.00007.x

Steinhauser, M. L., Olenchock, B. A., O'Keefe, J., Lun, M., Pierce, K. A., Lee, H., … Fazeli, P. K. (2018). The circulating metabolome of human starvation. *JCI Insight*, *3*(16), e121434. https://doi.org/10.1172/jci.insight.121434

Sun, J. S., Larter, N. K., Chahda, J. S., Rioux, D., Gumaste, A., & Carlson, J. R. (2018). Humidity response depends on the small soluble protein Obp59a in Drosophila. *eLife*, *7*, e39249. https://doi.org/10.7554/eLife.39249

Sun, Y.-L., Huang, L.-Q., Pelosi, P., & Wang, C.-Z. (2012). Expression in antennae and reproductive organs suggests a dual role of an odorant-binding protein in two sibling *Helicoverpa* species. *PLoS One*, *7*(1), e30040.

Tegoni, M., Campanacci, V., & Cambillau, C. (2004). Structural aspects of sexual attraction and chemical communlication in insects. *Trends in Biochemical Sciences*, *29*(5), 257–264.

Trott, O., & Olson, A. J. (2010). Software news and update AutoDock Vina: Improving the speed and accuracy of docking with a new scoring function, efficient optimization, and multithreading. *Journal of Computational Chemistry*, *31*(2), 455–461.

Tsuchihara, K., Fujikawa, K., Ishiguro, M., Yamada, T., Tada, C., Ozaki, K., & Ozaki, M. (2005). An odorant-binding protein facilitates odorant transfer from air to hydrophilic surroundings in the blowfly. *Chemical Senses*, *30*(7), 559–564. https://doi.org/10.1093/chemse/bji049

Untergasser, A., Cutcutache, I., Koressaar, T., Ye, J., Faircloth, B. C., Remm, M., & Rozen, S. G. (2012). Primer3-new capabilities and interfaces. *Nucleic Acids Research*, *40*(15), e115. https://doi.org/10.1093/nar/gks596

Usher, S., Han, L., Haslam, R. P., Michaelson, L. V., Sturtevant, D., Aziz, M., … Napier, J. A. (2017). Tailoring seed oil composition in the real world: Optimising omega-3 long chain polyunsaturated fatty acid accumulation in transgenic Camelina sativa. *Scientific Reports*, *7*, 6570. https://doi.org/10.1038/s41598-017-06838-0

Van der Horst, D. J., & Ryan, R. O. (2012). *Lipid transport* (pp. 317–345). New York: Academic Press.

van der Veen, J. N., Kennelly, J. P., Wan, S., Vance, J. E., Vance, D. E., & Jacobs, R. L. (2017). The critical role of phosphatidylcholine and phosphatidylethanolamine metabolism in health and disease. *Biochimica Et Biophysica Acta (BBA) - Biomembranes*, *1859*(9), 1558–1572. https://doi.org/10.1016/j.bbamem.2017.04.006

Vieira, F. G., & Rozas, J. (2011). Comparative genomics of the odorant-binding and chemosensory protein gene families across the Arthropoda: Origin and evolutionary history of the chemosensory system. *Genome Biology and Evolution*, *3*, 476–490. https://doi.org/10.1093/gbe/evr033

Wang, Z. J., Dong, Y. C., Desneux, N., & Niu, C. Y. (2013). RNAi silencing of the HaHMG-CoA reductase gene inhibits oviposition in the *Helicoverpa armigera* cotton bollworm. *PLoS One*, *8*(7), e67732. https://doi.org/10.1371/journal.pone.0067732

Xiao, S., Sun, J. S., & Carlson, J. R. (2019). Robust olfactory responses in the absence of odorant binding proteins. *eLife*, *8*, e51040. https://doi.org/10.7554/eLife.51040

Yan, S., Ni, H., Li, H., Zhang, J., Liu, X., & Zhang, Q. (2013). Molecular cloning, characterization, and mRNA expression of two cryptochrome genes in *Helicoverpa armigera* (Lepidoptera: Noctuidae). *Journal of Economic Entomology*, *106*(1), 450–462.

Ye, Z. F., Liu, X. L., Han, Q., Liao, H., Dong, X. T., Zhu, G. H., & Dong, S. L. (2017). Functional characterization of PBP1 gene in Helicoverpa armigera (Lepidoptera: Noctuidae) by using the CRISPR/Cas9 system. *Scientific Reports*, *7*(1). https://doi.org/10.1038/s41598-017-08769-2

Zhan, S., Zhang, W., Niitepõld, K., Hsu, J., Haeger, J. F., Zalucki, M. P., … Kronforst, M. R. (2014). The genetics of monarch butterfly migration and warning colouration. *Nature*, *514*(7522), 317–321. https://doi.org/10.1038/nature13812

Zhou, J. J. (2010). Odorant-binding proteins in insects. In G. Litwack (Ed.), *Vitamins and hormones: Pheromones* (vol. *83*, pp. 241–272). Academic Press.

Zhou, J. J., He, X. L., Pickett, J. A., & Field, L. M. (2008). Identification of odorant-binding proteins of the yellow fever mosquito Aedes aegypti: Genome annotation and comparative analyses. *Insect Molecular Biology*, *17*(2), 147–163. https://doi.org/10.1111/j.1365-2583.2007.00789.x

SUPPORTING INFORMATION

Additional supporting information may be found online in the Supporting Information section.

How to cite this article: Wang S, Minter M, Homem RA, et al. Odorant binding proteins promote flight activity in the migratory insect, *Helicoverpa armigera*. *Mol Ecol*. 2020;00:1–14. https://doi.org/10.1111/mec.15556